J Biomol NMR (2007) 39:17–29
DOI 10.1007/s10858-007-9167-5

ARTICLE

Quantitative Γ-HCNCH: determination of the glycosidic torsion angle χ in RNA oligonucleotides from the analysis of CH dipolar cross-correlated relaxation by solution NMR spectroscopy

Jörg Rinnenthal · Christian Richter · Jan Ferner · Elke Duchardt · Harald Schwalbe

Received: 5 March 2007 / Accepted: 22 May 2007 / Published online: 20 July 2007

Abstract A novel NMR pulse sequence is introduced to determine the glycosidic torsion angle χ in ^{13}C,^{15}N-labeled oligonucleotides. The quantitative Γ-HCNCH measures the dipolar cross-correlated relaxation rates $\Gamma^{DD,DD}_{C6H6,C1'H1'}$ (pyrimidines) and $\Gamma^{DD,DD}_{C8H8,C1'H1'}$ (purines). Cross-correlated relaxation rates of a ^{13}C,^{15}N-labeled RNA 14mer containing a cUUCGg tetraloop were determined and yielded χ-angles that agreed remarkably well with data derived from the X-ray structure of the tetraloop. In addition, the method was applied to the larger stemloop D (SLD) subdomain of the Coxsackievirus B3 cloverleaf 30mer RNA and the effect of anisotropic rotational motion was examined for this molecule. It could be shown that the χ-angle determination especially for nucleotides in the anti conformation was very accurate and the method was ideally suited to distinguish between the syn and the anti-conformation of all four types of nucleotides.

Keywords NMR spectroscopy · Isotope labeled RNA · χ-angle determination · Cross-correlated relaxation

Electronic Supplementary Material The online version of this article (doi:10.1007/s10858-007-9167-5) contains supplementary material, which is available to authorized users.

J. Rinnenthal · C. Richter · J. Ferner · E. Duchardt · H. Schwalbe (✉)
Institute for Organic Chemistry and Chemical Biology, Center for Biomolecular Magnetic Resonance, Johann Wolfgang Goethe-University, Max-von-Laue-Strasse 7, 60438 Frankfurt/Main, Germany
e-mail: schwalbe@nmr.uni-frankfurt.de

Introduction

The availability of isotope labeled RNA oligonucleotides (Batey et al. 1992; Nikonowicz et al. 1992; Quant et al. 1994; Batey et al. 1995) has stimulated the development of a large number of different heteronuclear NMR experiments (Varani and Tinoco 1991; Varani et al. 1996; Wijmenga 1998; Cromsigt et al. 2001; Fürtig et al. 2003) and allowed de-novo structure determination of sizeable RNA molecules by solution-state NMR spectroscopy. In comparison to the structure determination of proteins, where NOEs are the most important source of information, additional angular information is needed for RNA because the proton density is much lower than in proteins. Direct angular information can be obtained either from the analysis of homo- and heteronuclear ^3J coupling constants or from the interpretation of cross-correlated relaxation rates. Among the torsion angles of interest, the χ-angle determines the relative orientation of the nucleobase with respect to the ribose moiety, linking the nucleobases to the backbone scaffold of the RNA. The nucleobase can assume either the syn ($\chi \approx 40°$–$80°$) or the anti ($\chi \approx 180°$–$240°$) conformation. The analysis of populated torsion angles in RNA deposited in the data base shows a spread in χ of around 50° for purine and of around 30° for pyrimidine nucleotides. (see Fig. 2)

Using NMR-spectroscopy, the χ-angle can be determined by measurement of the ^3J(C2/4,H1′) and the ^3J(C6/8,H1′) coupling constants (Schwalbe et al. 1994; Trantirek et al. 2002; Munzarova and Sklenar 2003), using a Karplus parametrization. However, the accuracy of the angle determination depends on the quality of these Karplus parametrizations. The validity of the available parametrizations for RNA still remains to be investigated (Duchardt et al. 2004). More recently, cross-correlated relaxation Γ-rates were exploited to obtain structural

information in proteins (Reif et al. 1997; Pelupessy et al. 1999; Carlomagno et al. 2001; Schwalbe et al. 2001; Boisbouvier and Bax 2002; Kloiber et al. 2002; Zwahlen and Vincent 2002) and in oligosaccharides (Ilin et al. 2003). In oligonucleotides, the sugar pucker (Carlomagno et al. 1999; Felli et al. 1999; Richter et al. 1999), the angles of the sugar-phosphate backbone (Richter et al. 2000) and the χ-angle (Duchardt et al. 2004; Sychrovsky et al. 2005) can be determined from cross-correlated relaxation rates. In addition, if the structural parameters are known, cross-correlated relaxation Γ-rates can be used to analyze the dynamics of a biomacromolecule (Banci et al. 2001; Ravindranathan et al. 2003; Tugarinov and Kay 2004; Markwick et al. 2005; Wang et al. 2005).

Previously, we have reported the determination of the χ-angle from the measurement of nitrogen chemical shift anisotropy (N-CSA), C–H dipolar cross-correlated relaxation rates ($\Gamma^{CSA,DD}_{N1,C1'H1'}$ for pyrimidines and $\Gamma^{CSA,DD}_{N9,C1'H1'}$ for purines) (Duchardt et al. 2004). The method requires the knowledge of the size and the orientation of nitrogen (N1/N9) CSA tensors. These tensors have been determined for desoxymononucleotides by solid state NMR (Stueber and Grant 2002). However, the structural interpretation of cross-correlated relaxation rates that involve the chemical shift anisotropy as one relaxation mechanism is difficult, since little is known about the dependence of the CS tensors on either the sugar pucker mode or the χ-angle itself. Recent quantum mechanical calculations have indicated that the nitrogen chemical shift anisotropy can in fact be dependent on the χ-angle as well as on the conformation of the ribose moiety (Sychrovsky et al. 2005).

In this report, we therefore propose a new, CSA-independent method to determine the χ-angle based on the measurement of the dipolar cross-correlated relaxation rates $\Gamma^{DD,DD}_{C6H6,C1'H1'}$ and $\Gamma^{DD,DD}_{C8H8,C1'H1'}$ in a novel NMR experiment named the quantitative Γ-HCNCH. The method is applied to a 14mer cUUCGg RNA tetraloop and compared to the χ-angles derived from the previous analysis of the $\Gamma^{CSA,DD}_{N1,C1'H1'}$, $\Gamma^{CSA,DD}_{N9,C1'H1'}$ and the X-ray structure (Ennifar et al. 2000; Duchardt et al. 2004). Furthermore, we demonstrate the applicability of the novel method for a larger RNA, namely the stemloop D (SLD) subdomain of the Coxsackievirus B3 cloverleaf 30mer RNA (Ohlenschläger et al. 2004). In addition, we provide an easy to use $\Gamma^{DD,DD}(\chi)$ parametrization in order to facilitate the χ-angle determination.

Materials and methods

NMR spectroscopy

The measurements were performed using a uniformly ^{13}C, ^{15}N-labeled 14mer cUUCGg RNA tetraloop sample with the sequence 5′-PO_4^{2-}-PO_3^--PO_3^--GGCAC(UUCG)GUGC C-OH-3′. The secondary structure of the molecule is shown in Fig. 1A. The relevant chemical shifts for the resonance assignment were taken from Fürtig et al. (2004). The RNA was purchased from Silantes (Munich, Germany). The sample contained 0.7 mM RNA in 20 mM potassium phosphate, pH 6.4, 0.4 mM EDTA and 10% D_2O.

Additional measurements were performed on an adenosine, uridine-^{13}C, ^{15}N-labeled 30mer RNA (SLD of the CVB3 genomic RNA). The secondary structure of the molecule is shown in Fig. 1B (Ohlenschläger et al. 2004). The sample contained 1.2 mM RNA in 40 mM potassium phosphate, pH 6.2, 0.2 mM EDTA and 10% D_2O.

The NMR measurements were carried out on a Bruker 700 MHz spectrometer equipped with a 5 mm $^1H\{^{13}C/^{15}N\}$ z-axis-gradient cryogenic probe. Measurements were carried out at 298 K for the 14mer and 310 K for the 30mer. The data was processed and analyzed using the program TOPSPIN 1.3 (Bruker Biospin). Peak intensities were taken for the quantitative analysis of $\Gamma^{DD,DD}_{C6H6,C1'H1'}$ and $\Gamma^{DD,DD}_{C8H8,C1'H1'}$ according to Eq. 4. The stated error is equal to the RMSD of the multiple determined $\Gamma^{DD,DD}_{C6H6,C1'H1'}$ and $\Gamma^{DD,DD}_{C8H8,C1'H1'}$ rates recorded with different mixing times, different frequency labeling in t_1 (N1/9 or C1′) and two different pulse sequences that use signal detection either on the H1′ (Fig. 4) or the H8 (Supplementary Material).

MD simulation

A 5 ns molecular dynamics simulation of the 14mer was performed with the program CHARMM using the CHARMM27 nucleic acid force field (Foloppe and MacKerell Jr. 2000; MacKerell Jr and Banavali 2000). A recent X-ray structure (pdb ID 1F7Y) of the UUCG loop elongated by a standard A-form double strand of

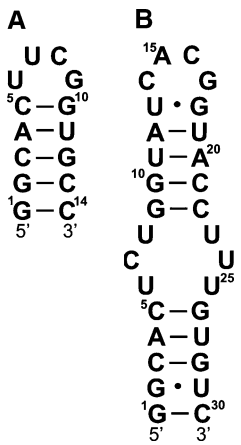

Fig. 1 (**A**) Secondary structure of the cUUCGg 14mer RNA. (**B**) Secondary structure of the uCACGg SLD 30mer RNA

appropriate sequence served as the starting structure for the simulation (Duchardt et al. 2004).

Simulations were carried out using periodic boundary conditions in a rhombic dodecahedron cut out of a cube with 50 Å side-length, filled with preequilibrated TPI3P water (Jorgensen et al. 1983). The system was neutralized with sodium counterions, which were placed manually by random replacement of water molecules. Non-bonded interactions were smoothly shifted to zero using a 12 Å cutoff. The pair-list of non-bonded interactions was generated using a 14 Å cutoff, and updated whenever any atom had moved >1 Å since the last list update. The calculation of the trajectory took place under constant pressure conditions using the Langevin piston method (Feller et al. 1995) with a check every 4 ps that the average temperature remained within ±5 K of 298 K. Conformations of the system were saved every 0.2 ps for further analysis. χ-angle extraction was performed using CHARMM input scripts. The first 500 ps of the trajectory were not considered in the analysis.

Theory

For a RNA macromolecule that shows isotropic rotational tumbling in solution, the $\Gamma^{DD,DD}_{C6H6,C1'H1'}$ and $\Gamma^{DD,DD}_{C8H8,C1'H1'}$ cross-correlated relaxation rates are given by

$$\begin{aligned}\Gamma^{DD,DD}_{C6H6,C1'H1'} &\equiv \frac{1}{5}\frac{\gamma_H^2\gamma_C^2}{r^3_{C6H6}r^3_{C1'H1'}}\left(\frac{\mu_0}{4\pi}\right)^2\hbar^2 \\ &\times\left(S^{DD,DD}_{C6H6,C1'H1'}\right)^2\left(3\cos^2\theta_{C6H6,C1'H1'}-1\right)\tau_c \\ \Gamma^{DD,DD}_{C8H8,C1'H1'} &\equiv \frac{1}{5}\frac{\gamma_H^2\gamma_C^2}{r^3_{C8H8}r^3_{C1'H1'}}\left(\frac{\mu_0}{4\pi}\right)^2\hbar^2 \\ &\times\left(S^{DD,DD}_{C8H8,C1'H1'}\right)^2\left(3\cos^2\theta_{C8H8,C1'H1'}-1\right)\tau_c\end{aligned} \quad (1)$$

where γ_H and γ_C are the gyromagnetic ratios for the hydrogen and carbon nuclei, $r_{C6H6(C8H8)}$ and $r_{C1'H1'}$ are the lengths of the $\overrightarrow{C6H6}(\overrightarrow{C8H8})$ and $\overrightarrow{C1'H1'}$ bond vectors (Fig. 3C) which are set to 1.104 and 1.090 Å, respectively (Ying et al. 2006), μ_0 is the magnetic susceptibility of the vacuum, τ_c is the isotropic rotational correlation time of the molecule, $\hbar$ is the Planck constant divided by 2π, $S^{DD,DD}_{C6H6,C1'H1'}$ ($S^{DD,DD}_{C8H8,C1'H1'}$) are the cross-correlated order parameters for internal motion and $\theta_{C6H6,C1'H1'}$ ($\theta_{C8H8,C1'H1'}$) are the projection angles between the $\overrightarrow{C6H6}(\overrightarrow{C8H8})$ and the $\overrightarrow{C1'H1'}$ bond vectors in pyrimidine and purine nucleotides, respectively. The projection angle $\theta_{C6H6,C1'H1'}$ ($\theta_{C8H8,C1'H1'}$) is a function of the glycosidic torsion angle χ. It follows that also $\Gamma^{DD,DD}_{C6H6,C1'H1'}$ and $\Gamma^{DD,DD}_{C8H8,C1'H1'}$ can be related to torsion angle χ by application of basic geometric considerations. The derivation of this relationship is given in the supplementary material (S2). From this, a parametrization similar to the Karplus equations for J couplings can be deduced also for $\Gamma^{DD,DD}_{C6H6,C1'H1'}$ and $\Gamma^{DD,DD}_{C8H8,C1'H1'}$. This parametrization is only dependent on χ, the order parameter $(S^{DD,DD}_{C6H6,C1'H1'})^2$ or $(S^{DD,DD}_{C8H8,C1'H1'})^2$ and τ_c.

$$\begin{aligned}\Gamma^{DD,DD}_{C6H6,C1'H1'} &= 4.1370\tau_c\left(S^{DD,DD}_{C6H6,C1'C1'}\right)^2 10^9[A\cos(\chi-59.01) \\ &+B\cos(2\chi-118.01)+C] \\ \Gamma^{DD,DD}_{C8H8,C1'H1'} &= 4.1370\tau_c\left(S^{DD,DD}_{C8H8,C1'C1'}\right)^2 10^9[A\cos(\chi-59.01) \\ &+B\cos(2\chi-118.01)+C]\end{aligned} \quad (2)$$

The parameters A, B and C are summarized in Table 1 for purines and pyrimidines and are shown in Fig. 2 for the 14mer RNA assuming an isotropic overall rotational correlation time τ_c equal to 2.31 ns (Duchardt and Schwalbe 2005). Since the parametrizations for the nucleobases C and U are almost identical to each other and also the parametrizations for the nucleobases G and A, it makes sense to summarize the different parametrization curves for the four different kinds of nucleotides to two different parametrization curves distinguishing only between purines and pyrimidines. The exact parametrizations for the nucleobases C, U, A and G are given in the supplementary material (Table S1). For the cross-correlated order parameters $(S^{DD,DD}_{C8H8,C1'H1'})^2$ and $(S^{DD,DD}_{C6H6,C1'H1'})^2$ (Table 2) we used a value derived from the autocorrelated order parameters derived from ^{13}C relaxation analysis (Duchardt and Schwalbe 2005) as approximation for the cross-correlated order parameters. As pointed out by Bodenhausen and coworkers, this approach is valid if one assumes fast uncorrelated motion of the $\overrightarrow{C6H6}(\overrightarrow{C8H8})$ bond vectors with respect to the $\overrightarrow{C1'H1'}$ bond vectors (Vugmeyster et al. 2004).

For the cUUCGg 14mer RNA the assumption of isotropic rotational diffusion is valid since the rotational diffusion anisotropy A is small (A = 1.35) (Duchardt and Schwalbe 2005). For molecules that have a rather extended shape, as it is the case for the SLD 30mer RNA (Fig. 1B), the effect of anisotropic rotational tumbling cannot be neglected. Therefore, we analyzed the $\Gamma^{DD,DD}_{C6H6,C1'H1'}$ and $\Gamma^{DD,DD}_{C8H8,C1'H1'}$ rates by taking the size and the orientation of the axially symmetric rotational diffusion tensor into

Table 1 Parameters for the calculation of the $\Gamma^{DD,DD}_{C6H6,C1'H1'}$ and $\Gamma^{DD,DD}_{C8H8,C1'H1'}$ according to equation (2)

	A	*B*	*C*
Purines	0.583	1.191	0.226
Pyrimidines	0.801	1.015	0.093

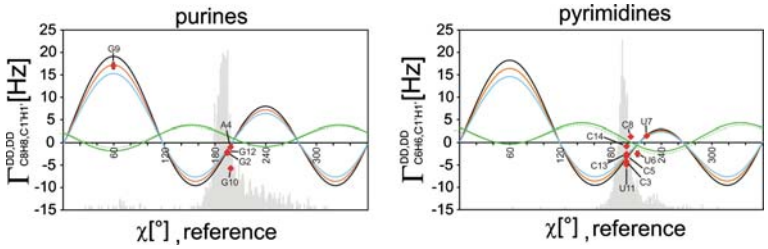

Fig. 2 $\Gamma^{DD,DD}_{C8H8,C1'H1'}(\chi)$ for purines and $\Gamma^{DD,DD}_{C6H6,C1'H1'}(\chi)$ for pyrimidines, curves are shown for $(S^{DD,DD}_{C8H8,C1'H1'})^2$ and $(S^{DD,DD}_{C6H6,C1'H1'})^2$ equal to 0.8 (light blue), 0.9 (orange) and 1.0 (black). τ_c was set to 2.31 ns (Duchardt and Schwalbe 2005) for the 14mer at 298 K. In addition, the experimental $\Gamma^{DD,DD}_{C6H6,C1'H1'}$ and $\Gamma^{DD,DD}_{C8H8,C1'H1'}$ from the 14mer RNA are plotted against the reference χ-angles (Duchardt et al. 2004) (red squares). $\Gamma^{CSA,DD}_{N1,C1'H1'}$ for pyrimidines and $\Gamma^{CSA,DD}_{N9,C1'H1'}$ for purines are illustrated as green solid (guanine, cytosine) and dashed (adenine, uracil) lines, respectively. The gray bars represent the χ-angle distribution in the RNA fraction of the large ribosomal subunit (PDB entry 1FFK (Ban et al. 2000))

Table 2 $\Gamma^{DD,DD}_{C6H6,C1'H1'}$, $\Gamma^{DD,DD}_{C8H8,C1'H1'}$ and the corresponding χ-angles in comparison to the reference (crystal structure), the χ-angles extracted from the $\Gamma^{CSA,DD}_{N1,C1'H1'}$, $\Gamma^{CSA,DD}_{N9,C1'H1'}$, and the ^3J(C,H)-coupling constants (Duchardt et al. 2004)

Nucleotide	(Hz)		χ[°]	χ[°]	χ[°]	χ[°]	χ[°]
	$\Gamma^{DD,DD}_{C6H6,C1'H1'}$ / $\Gamma^{DD,DD}_{C8H8,C1'H1'}$	$(S^{DD,DD}_{C6H6,C1'H1'})^2$ / $(S^{DD,DD}_{C8H8,C1'H1'})^2$	$\Gamma^{DD,DD}_{C6H6,C1'H1'}$ / $\Gamma^{DD,DD}_{C8H8,C1'H1'}$	(MD simulation)	^3J(C,H)	$\Gamma^{CSA,DD}_{N1,C1'H1'}$ / $\Gamma^{CSA,DD}_{N9,C1'H1'}$	(X-ray)
G1							194.8 ± 4.4
G2	–2.3 ± 0.4	0.959	192.4 ± 1.4	197.5 ± 7.8	192 ± 2	205 ± 1	194.8 ± 4.4
C3	–4.3 ± 0.1	0.926	193.7 ± 0.4	202.4 ± 7.4		203 ± 1	198.4 ± 3.1
A4	–0.9 ± 0.1	0.968	196.3 ± 0.4	198.9 ± 7.7	198.5 ± 1.5	207 ± 1	198.2 ± 3.5
C5	–3.1 ± 0.3	0.920	198.8 ± 1.3	196.7 ± 7.3	191 ± 8	201 ± 1	197.85
U6	–2.5 ± 0.6	0.935	201.2 ± 2.5	204.4 ± 7.5	196.5 ± 4.5	221	211.03
U7	1.5 ± 0.2	0.777	223.6 ± 2.1	237.2 ± 17.6	217.5 ± 9.5	209 ± 4	222.23
C8	1.3 ± 0.2	0.880	221.6 ± 1.5	204.6 ± 10.2	210.5 ± 6.5	218 ± 2	202.64
G9	17.0 ± 0.6	0.932	48.6 ± 5.2	27.3 ± 7.1	44 ± 4	57 ± 19	56.66
(G9)			69.4 ± 5.2				
G10	–5.7 ± 0.4	0.943	180.0 ± 1.6	191.2 ± 7.7	215.5 ± 13.5	201 ± 2	198.24
U11	–5.0 ± 0.3	0.952	190.9 ± 1.4	199.1 ± 7.8		195	198.2 ± 3.0
G12	–2.1 ± 0.4	0.952	193.0 ± 1.1	188.1 ± 7.9	192 ± 4	207 ± 1	194.8 ± 4.4
C13	–2.6 ± 0.2	0.938	201.4 ± 0.9	200.3 ± 7.2	189.5 ± 3.5	202 ± 1	198.4 ± 3.1
C14	–0.9 ± 0.3	0.867	208.8 ± 1.3	208.9 ± 11.7	198 ± 5	211 ± 1	198.4 ± 4.4

The reference angles for the nucleotides C5–G10 are extracted from the crystal structure (pdb ID 1F7Y) (Ennifar et al. 2000), the other reference values are mean values for the A-Form RNA obtained as described previously (Duchardt et al. 2004). The $\Gamma^{DD,DD}_{C6H6,C1'H1'}$ and $\Gamma^{DD,DD}_{C8H8,C1'H1'}$ were determined several times with different mixing times T_M (20, 30 ms). $(^{cross}S^{DD,DD}_{C6H6,C1'H1'})^2$ and $(^{cross}S^{DD,DD}_{C8H8,C1'H1'})^2$ were estimated from the autocorrelated order parameters (Ferner and Schwalbe) as a product of $\sqrt{(^{auto}S_{C6H6,C6H6})^2} * \sqrt{(^{auto}S_{C1'H1',C1'H1'})^2}$ and $\sqrt{(^{auto}S_{C8H8,C8H8})^2} * \sqrt{(^{auto}S_{C1'H1',C1'H1'})^2}$ respectively. $(S^{DD,DD}_{C6H6,C1'H1'})^2$ and $(S^{DD,DD}_{C8H8,C1'H1'})^2$ were used for determination of the χ-angles. There is only one remaining possibility for the χ-angle lying close to the reference value (Ennifar et al. 2000; Duchardt et al. 2004) for each nucleotide in the anti conformation. In contrast, two values for the χ-angle remain possible for the nucleotide G9 which assumes the syn conformation due to degeneracy of the parametrization curve

account. The mathematical relations for the anisotropic case are given in section S4 of the supplementary material.

Pulse sequence

The quantitative Γ-HCNCH experiment (Fig. 4) is derived from the HCN and HCNCH experiments (Sklenar et al. 1993a, b; Fiala et al. 1998; Sklenar et al. 1998). It is designed to transfer coherence in a directed manner from H6 (H8) to H1′, where the signal is detected. The scheme is similar to that in the quantitative Γ-HCCH experiment (Felli et al. 1999; Millet et al. 1999). The coherence at time point **a** is created via three successive INEPT steps transferring the coherence from H6 (H8) to C1′. During the

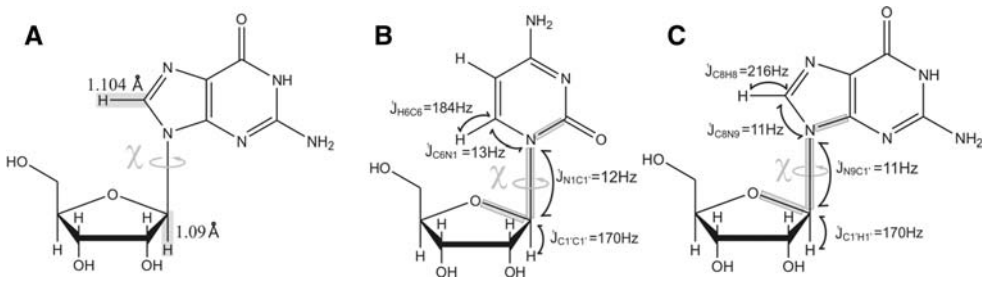

Fig. 3 In (**A**), the bond vectors relevant for the derivation of projection angles from $\Gamma^{DD,DD}_{C8H8,C1'H1'}$ are marked in gray. (**B**) and (**C**) show the magnitude of the experimentally determined ^1J scalar couplings used to transfer the magnetization from H6(8) to H1′ (Fiala et al. 2004) in the case of pyrimidines and purines in the quantitative Γ-HCNCH experiment. The bonds underlaid with gray define the χ-angle

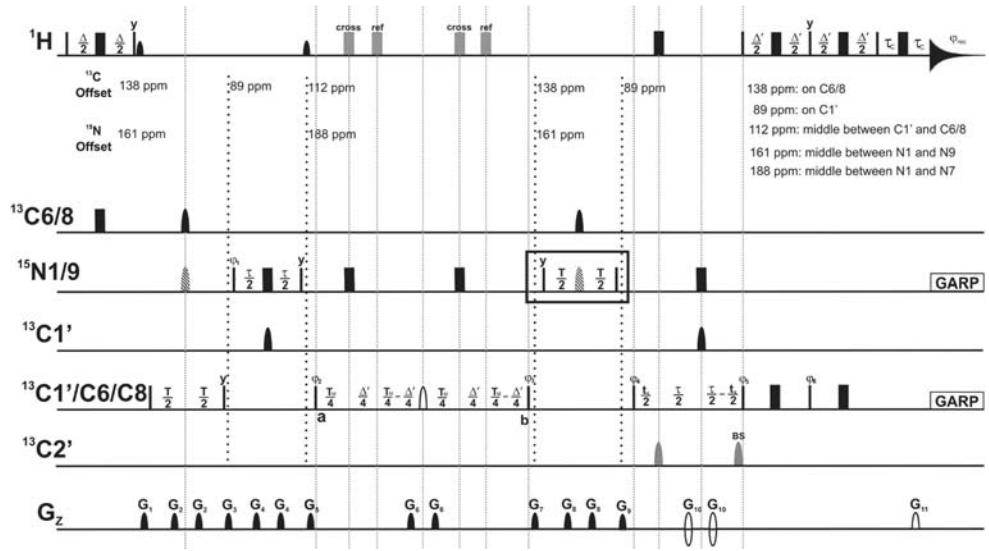

Fig. 4 Pulse sequence of the quantitative Γ-HCNCH experiment. Narrow and wide filled bars correspond to rectangular 90° and 180° pulses, respectively. Selective pulses and gradients are indicated as semi-ellipses. The default pulse phase is x. The pulse sequences were optimized on a Bruker spectrometer with the Bruker typical phase settings (Roehrl et al. 2005). The reference and the cross experiment are summarized in one pulse sequence scheme. The gray wide filled bars correspond to 180° pulses applied on the proton channel either in the cross or the reference experiment, as indicated. Two water flipback pulses are applied after the INEPT steps before the mixing time T_M (small black semi-ellipses). Two selective off-resonant pulses on C2′ during the carbon constant time chemical shift evolution are shown in gray. Fixed delays are adjusted as follows: $\Delta' = 2.94\,\text{ms}(1/(2^{*1}J_{H1'C1'}))$, $\Delta = 2.5\,\text{ms}(1/(2^{*1}J_{H6(8)C6(8)}))$, $T = 32\,\text{ms}(1/(2^{*1}J_{C6(8)N1(9)}))$, $\tau = 36\,\text{ms}((1/2^{*1}J_{N1(9)C1'}))$. T_M is the variable relaxation period. The proton carrier frequency is centered at the water frequency (4.7 ppm). The carbon and the nitrogen carrier frequencies change during the course of the experiment as indicated by vertical dashed lines. The values of the ^{13}C and ^{15}N offset at every time point are given, respectively. At 700 MHz, band selective pulses are set as follows: 180° Q3 Gaussian cascade (Emsley and Bodenhausen 1992) 2 ms (black semi-ellipse), 180° Q3 Gaussian cascade 1 ms (gray semi-ellipse), 180° Q3 Gaussian cascade 0.5 ms (hatched semi-ellipse), 180° Reburp (Geen and Freeman 1991) 2.53 ms with maxima on C1′ and C6/8 (open semi-ellipse), 90° square pulses 1 ms (small black semi-ellipse, water flipback). Asynchronous GARP decoupling (Shaka et al. 1985) is used to suppress heteronuclear scalar couplings during acquisition. The pulse field gradients of 1 ms length have a smoothed chirp amplitude (Bruker Topspin 2.0, 2006). They are applied along the z-axis and have the following strengths: G_1:–40%, G_2:25%, G_3:50%, G_4:20%, G_5:–40%, G_6:20%, G_7:65%, G_8:20%, G_9:50%, G_{10}:40%, G_{11}:20.1%. 100% of gradient strength corresponds to 55 Gauss/cm. Phase cycling: $\varphi_1 = x, -x$; $\varphi_2 = 8(x), 8(-x)$; $\varphi_3 = 16(y), 16(-y)$; $\varphi_4 = 4(y), 4(-y)$; $\varphi_5 = (2x), 2(-x)$; $\varphi_6 = -2(y), 2(y)$; $\varphi_{rec} = x, 2(-x), x, -x, 2(x), -x$. G_{10} and ϕ_6 are modulated according to echo/antiecho modulation in the ω_1 dimension using sensitivity enhancement (Kay et al. 1992). At time point **a**, the coherence $H6(8)_zC6(8)_yC1'_yN1(9)_z$ is created and converts during T_M into the coherence $H1'_zC6(8)_xC1'_xN1(9)_z$ at time point **b**. If additional chemical shift dispersion is needed, a N1(9) constant time evolution period can be introduced during the first refocusing INEPT step as indicated by the black box. In this case, ϕ_4 is incremented in a States-TPPI (Marion et al. 1989) manner to achieve quadrature detection in the N1(N9) dimension

mixing time T_M, the generated coherence $8H6(8)_zC6(8)_yC1'_yN1(9)_z$ at time point **a** evolves into the coherence $8H1'_zC6(8)_xC1'_xN1(9)_z$ at time point **b**. Frequency labeling of C1′ occurs in a constant time manner during the second refocusing INEPT step of the transfer to H1′ after the mixing period T_M. If additional chemical shift resolution is needed, a constant time N1(9) chemical shift evolution period can be used during the first refocusing INEPT step alternatively to the C1′ chemical shift evolution period. The coherence transfer could also be performed starting at H1′. Experimental details for the pulse sequence with reverted coherence transfer are given in the Supplementary Material (S3). The analysis of cross-correlated relaxation rates given later is based on both pulse sequences with different mixing times T_M, respectively. The stated error is the RMSD calculated from six independent measurements with both pulse sequences using different mixing times T_M (supplementary material section S1, Fig. S1). The various INEPT delays for magnetization transfer are optimized taking into account the relevant coupling constants which are depicted in Fig. 3.

Two different experiments are recorded, a cross and a reference experiment. In the cross experiment, the coherence selected at time point **b** is $\sinh(\Gamma^{DD,DD}_{C6H6,C1'H1'}T_M)$ (or $(\sinh\Gamma^{DD,DD}_{C8H8,C1'H1'}T_M)$) modulated. In the reference experiment, the selected coherence is modulated by $\cosh(\Gamma^{DD,DD}_{C6H6,C1'H1'}T_M)^*\sin(\pi J_{C6H6}\Delta')$ (or $\cosh(\Gamma^{DD,DD}_{C8H8,C1'H1'}T_M)^*\sin(\pi J_{C8H8}\Delta')$ for purines).

The measured cross-correlation effect increases at longer mixing times T_M but is also counteracted by auto-correlated relaxation effects. The optimal sensitivity in the cross experiment was achieved using a mixing time T_M in the range of 20-30 ms for the 14mer RNA and between 10 ms and 15 ms for the 30mer RNA.

In the case of pyrimidines, the evolution of the excited double and zero quantum coherence $8H6_zC6_yC1'_yN1_z$ during T_M is given by

$$\begin{aligned}
8H6_zC6_yC1'_yN1_z \rightarrow\ & 8H6_zC6_yC1'_yN1_z[\cosh(\Gamma^{DD,DD}_{C6H6,C1'H1'}T_M)\\
& \cos(\pi J_{C6H6}\Delta')\cos(\pi J_{C1'H1'}\Delta')\\
& +\sinh(\Gamma^{DD,DD}_{C6H6,C1'H1'}T_M)\sin(\pi J_{C6H6}\Delta')\sin(\pi J_{C1'H1'}\Delta')]\\
& +8H1'_zC6_xC1'_xN1_z[\sinh(\Gamma^{DD,DD}_{C6H6,C1'H1'}T_M)\cos(\pi J_{C6H6}\Delta')\\
& \cos(\pi J_{C1'H1'}\Delta')+\cosh(\Gamma^{DD,DD}_{C6H6,C1'H1'}T_M)\\
& \sin(\pi J_{C6H6}\Delta')\sin(\pi J_{C1'H1'}\Delta')]
\end{aligned} \tag{3}$$

Note that in the case of purines, the nomenclature of the involved nuclei is different (H8 → H6, C8 → C6, N9 → N1). During the mixing time T_M, the coherence $8H6(8)_zC6(8)_yC1'_yN1(9)_z$ converts into the coherence $8H1'_zC6(8)_xC1'_xN1(9)_z$ that is selected at the end of the mixing time T_M; in the reference experiment, this transfer is accomplished via scalar coupling, in the cross experiment, coherence transfer is accomplished via cross-correlated relaxation.

In the reference experiment with $\Delta' = 1/(2^*J_{C1'H1'})$, the intensity of the peak I^{ref} is proportional to $\cosh(\Gamma^{DD,DD}_{C6H6,C1'H1'}T_M)\sin(\pi J_{C6H6}\Delta')$. In the cross experiment, the J_{CH} scalar coupling is completely refocused because of $\Delta' = 0$ and the intensity of the peak I^{cross} is modulated by $\sinh(\Gamma^{DD,DD}_{C6H6,C1'H1'}T_M)$. Consequently, division of the two intensities yields an expression for the cross-correlated relaxation rate given by the following equation:

$$\begin{aligned}
\Gamma^{DD,DD}_{C6H6,C1'H1'} &= T_M^{-1}\tanh^{-1}\left(\frac{ns^{ref}I^{cross}\sin(\pi J_{C6H6}\Delta')}{ns^{cross}I^{ref}}\right)\\
\Gamma^{DD,DD}_{C8H8,C1'H1'} &= T_M^{-1}\tanh^{-1}\left(\frac{ns^{ref}I^{cross}\sin(\pi J_{C8H8}\Delta')}{ns^{cross}I^{ref}}\right)
\end{aligned} \tag{4a}$$

In Eq. 4, T_M represents the length of the double and zero quantum coherence mixing time, ns^{ref} and ns^{cross} are the number of transients recorded in the cross and the reference experiment. I^{cross} and I^{ref} are the intensities of the peaks extracted from the cross and the reference experiment and the $\sin(\pi J_{C6H6}\Delta')$ and $\sin(\pi J_{C8H8}\Delta')$ terms with $\Delta' = 2.94$ ms take the different scalar couplings in purines (216 Hz) and pyrimidines (184 Hz) into account. An error of ±5 Hz in the J_{C8H8} of the purines leads to a relative error for the $\Gamma^{DD,DD}_{C8H8,C1'H1'}$ of 1.3%. For purines assuming the syn conformation this error calculates to 0.26 Hz, assuming a τ_c of 2.31 ns. For the purines in the anti conformation the error is too small to have any effect since the absolute rate is very small in these cases. An error of ±5 Hz in the J_{C6H6} of the pyrimidines and in the $J_{C1'H'}$ are also too small and can therefore be neglected.

There is the need to discuss to which extent cross-correlated relaxation mechanism other than $\Gamma^{DD,DD}_{C6H6,C1'H1'}$ ($\Gamma^{DD,DD}_{C8H8,C1'H1'}$) contribute to the relaxation of the double and zero quantum coherence operators during T_M. Most other cross-correlated relaxation mechanisms create coherences with a different number of product operators or with different phases. Consequently, they are not selected in the cross experiment and are removed by both phase cycling and pulse field gradients.

Evolution of the cross-correlated relaxation rates $\Gamma^{DD,CSA}_{C6H6,C1'}$, $\Gamma^{DD,CSA}_{C8H8,C1'}$, $\Gamma^{DD,CSA}_{C1'H1',C6}$ and $\Gamma^{DD,CSA}_{C1'H1',C8}$ is suppressed by the π-pulses on ^{1}H in the cross experiment. However, for the time the scalar coupling evolves (2.94 ms) in the reference experiment these rates evolve, too. Of course, the desired rates $\Gamma^{DD,DD}_{C6H6,C1'H1'}$ and $\Gamma^{DD,DD}_{C8H8,C1'H1'}$ evolve over the entire mixing time, while the $\Gamma^{DD,CSA}_{C6H6,C1'}$, $\Gamma^{DD,CSA}_{C8H8,C1'}$ $\Gamma^{DD,CSA}_{C1'H1',C6}$ and $\Gamma^{DD,CSA}_{C1'H1',C8}$ rates only evolve for 2.94 ms, no matter how long the mixing time is. Therefore the "apparent" $\Gamma^{DD,CSA}_{C1'H1',C6}$ and $\Gamma^{DD,CSA}_{C1'H1',C8}$ rates decrease with longer mixing times T_M.

The intensity terms of the reference experiment enter into the calculation (Eq. 4b) as cosh-modulated terms. We simulated the curves for the $\Gamma^{DD,CSA}_{C1'H1',C6}$ and $\Gamma^{DD,CSA}_{C1'H1',C8}$ and calculated the error for the syn and anti conformations separately. The maximum values are $\Gamma^{DD,CSA}_{C1'H1',C6} = 13.4$ Hz and $\Gamma^{DD,CSA}_{C1'H1',C8} = 11.0$ Hz for nucleotides in the syn conformation. In the anti conformation, these rates are smaller and depend on the χ-angle. For the $\Gamma^{DD,CSA}_{C6H6,C1'}$ and $\Gamma^{DD,CSA}_{C8H8,C1'}$ rates we took the maximum possible value to estimate the error caused by these rates. $\Gamma^{DD,CSA}_{C6H6,C1'}$ and $\Gamma^{DD,CSA}_{C8H8,C1'}$ can assume a maximum value of 3.0 Hz. Since the CSA of the C1′ is quite small, this error is negligible small.

Taking the $\Gamma^{DD,CSA}_{C1'H1',C6}$ and $\Gamma^{DD,CSA}_{C1'H1',C8}$ rates into account, this Eq. 4 can be rewritten as:

$$\frac{\sinh(\Gamma^{DD,DD}_{C6H6,C1'H1'} * T_M)}{\cosh((\Gamma^{DD,DD}_{C6H6,C1'H1'} * T_M + \Gamma^{DD,CSA}_{C1'H1',C6} * 2.94\,ms))} = \left(\frac{ns^{ref} I^{cross} \sin(\pi J_{C6H6}\Delta')}{ns^{cross} I^{ref}}\right)$$
$$\frac{\sinh(\Gamma^{DD,DD}_{C8H8,C1'H1'} * T_M)}{\cosh((\Gamma^{DD,DD}_{C8H8,C1'H1'} * T_M + \Gamma^{DD,CSA}_{C1'H1',C8} * 2.94\,ms))} = \left(\frac{ns^{ref} I^{cross} \sin(\pi J_{C8H8}\Delta')}{ns^{cross} I^{ref}}\right) \quad (4b)$$

Equation 4b and simulated $\Gamma^{DD,CSA}_{C1'H1',C6}$ and $\Gamma^{DD,CSA}_{C1'H1',C8}$ rates are the basis for the error calculation. As long as the argument of the cosh function is very small (<0.1) the error is also small since the slope of the cosh function is very small for small arguments.

Because the $\Gamma^{DD,CSA}_{C1'H1',C6}$ and $\Gamma^{DD,CSA}_{C1'H1',C8}$ rates influence the cosh-modulated term of the reference experiment and only evolve for 2.94 ms, the error depends on the mixing time. For a mixing time of 30 ms, the maximum error caused by the $\Gamma^{DD,CSA}_{C1'H1',C6}$ and $\Gamma^{DD,CSA}_{C1'H1',C8}$ rates calculates to 2.2%. This is equal to 0.4 Hz for the G9 residue of the 14mer which assumes syn conformation around χ. The error caused by the $\Gamma^{DD,CSA}_{C1'H1',C6}$ and $\Gamma^{DD,CSA}_{C1'H1',C8}$ rates for nucleotides assuming the anti conformation is negligible small (<0.03 Hz for the 14mer RNA).

Results and discussion

cUUCGg 14mer RNA

The quantitative Γ-HCNCH experiment for the determination of the glycosidic torsion angle χ was applied to a 14mer cUUCGg tetraloop RNA (Fig. 1A). For this tetraloop-hairpin, chemical shifts of almost all the nuclei are known (Fürtig et al. 2004). The RNA consists of a stem region with five canonical base pairs and a structured loop region with one nucleotide (G9) assuming the syn conformation (Allain and Varani 1995; Ennifar et al. 2000). The molecule is soluble and monomeric at high concentrations. In addition, the $\Gamma^{CSA,DD}_{N1,C1'H1'}$ and $\Gamma^{CSA,DD}_{N9,C1'H1'}$ rates have been measured before to determine the χ-angle for this molecule (Duchardt et al. 2004) and the results presented here can be directly compared to these data.

There are two structures of cUUCGg tetraloops published so far, one crystal structure (pdb ID 1F7Y (Ennifar et al. 2000)) and one NMR ensemble (pdb ID 1HLX (Allain and Varani 1995)). The results presented here are compared to the values for χ extracted from the crystal structure, to the $\Gamma^{CSA,DD}_{N1,C1'H1'}$ and $\Gamma^{CSA,DD}_{N9,C1'H1'}$-rates and to ^3J(C,H) coupling constants determined previously (Duchardt et al. 2004).

Figure 2 shows the dependencies $\Gamma^{DD,DD}_{C6H6,C1'H1'}(\chi)$ and $\Gamma^{DD,DD}_{C8H8,C1'H1'}(\chi)$. These curves demonstrate that an unambiguous distinction between the syn and the anti conformation is possible for all four types of nucleotides. In addition, the slope of the curve around the anti conformation is steep and accompanied with a sign change. Since the accuracy of the angle determination is determined by the slope of the parametrization curve, the angle determination is very precise for nucleotides assuming the anti conformation. Figure 2 also shows the previously introduced $\Gamma^{CSA,DD}_{N1,C1'H1'}$ and $\Gamma^{CSA,DD}_{N9,C1'H1'}$, these are much smaller, but show a different absolute sign in the interesting conformational regions the angle χ commonly adopts.

The spectra of the quantitative Γ-HCNCH reference and cross experiment are shown in Fig. 5. $\Gamma^{DD,DD}_{C6H6,C1'H1'}$ and $\Gamma^{DD,DD}_{C8H8,C1'H1'}$ are obtained from the intensities of the peaks from the cross and the reference spectra according to Eq. 4. The rates were determined several times at different mixing times T_M (Table 2). The margin of error for rates obtained from multiple experiments lies between 0.1 Hz and 0.6 Hz (Table 2), which is very accurate considering the range of values that can be observed for $\Gamma^{DD,DD}_{C6H6,C1'H1'}$ and $\Gamma^{DD,DD}_{C8H8,C1'H1'}$ of up to 19 Hz. The correlation of $\Gamma^{DD,DD}_{C6H6,C1'H1'}$ and $\Gamma^{DD,DD}_{C8H8,C1'H1'}$ with the χ-angles extracted from the X-ray structure (pdb ID 1F7Y) (Ennifar et al. 2000) is shown in Fig. 2. It can be seen that the experimental $\Gamma^{DD,DD}_{C6H6,C1'H1'}$ and $\Gamma^{DD,DD}_{C8H8,C1'H1'}$ rates are in remarkable agreement with the predicted rates. The determined $\Gamma^{DD,DD}_{C6H6,C1'H1'}$ and $\Gamma^{DD,DD}_{C8H8,C1'H1'}$ rates were translated into χ-angles using the theoretically derived $\Gamma^{DD,DD}_{C6H6,C1'H1'}(\chi)$ and $\Gamma^{DD,DD}_{C8H8,C1'H1'}(\chi)$ dependence (Eq. 2, Table 1). The correlation of the χ-angles obtained from the X-ray structure (pdb ID 1F7Y) (Ennifar et al. 2000) and the analyzed $\Gamma^{DD,DD}_{C6H6,C1'H1'}$ and $\Gamma^{DD,DD}_{C8H8,C1'H1'}$ (Table 2, Fig. 6A) yields an RMSD of 9.2° for all nucleotides. The correlation between χ-angles extracted from the $\Gamma^{CSA,DD}_{N1,C1'H1'}$ and $\Gamma^{CSA,DD}_{N9,C1'H1'}$ (Duchardt et al. 2004) with the χ-angles obtained by analyzing the $\Gamma^{DD,DD}_{C6H6,C1'H1'}$ and $\Gamma^{DD,DD}_{C8H8,C1'H1'}$ yields an RMSD of 10.1° (Table 2, Fig. 6B). It appears that the χ-angles obtained from the $\Gamma^{DD,DD}_{C6H6,C1'H1'}$ and $\Gamma^{DD,DD}_{C8H8,C1'H1'}$ tend to be systematically smaller than the ones determined by the $\Gamma^{CSA,DD}_{N1,C1'H1'}$ and $\Gamma^{CSA,DD}_{N9,C1'H1'}$. When taking only the cytidines into account the two methods are in very good agreement with a RMSD of

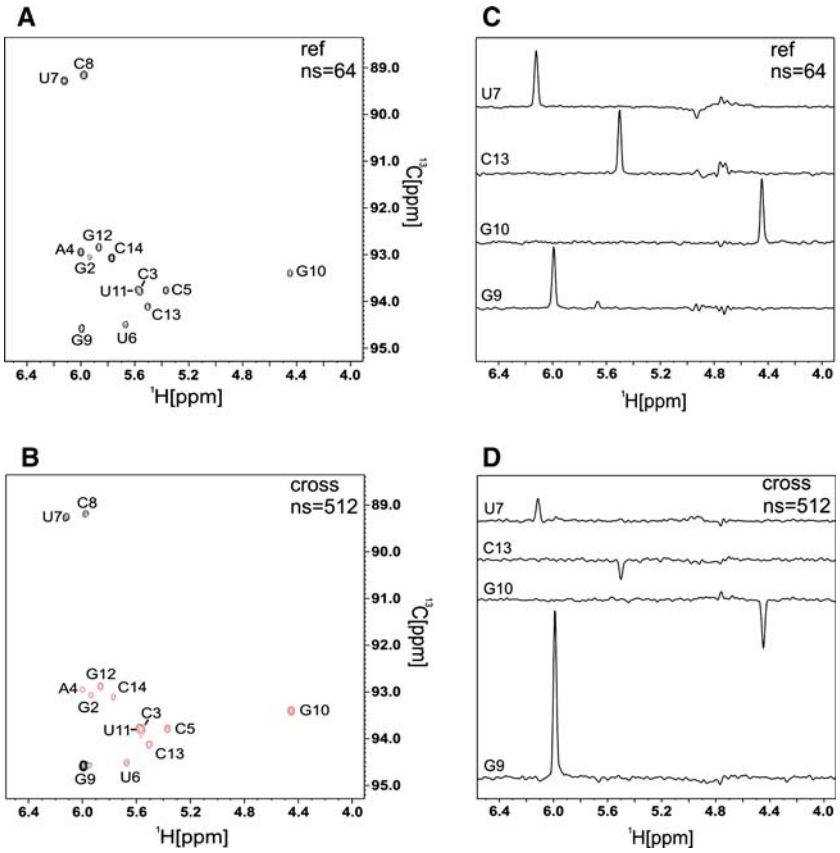

Fig. 5 Spectra of the quantitative Γ-HCNCH experiment for the 14mer RNA. The reference experiment is shown in (**A**), the cross experiment in (**B**). Negative signals are shown in red. (**C**, **D**): Selected 1D slices taken from the reference (**A**) and the cross experiment (**B**). The spectra were recorded on a 700 MHz spectrometer. The reference and the cross experiment were recorded using 64 increments in the C1′ dimension and 64 scans for each increment in the reference experiment. The cross experiment was recorded with 512 scans per increment. T_M was set to 30 ms. The reference experiment was recorded in 2 h and the cross experiment in 16 h

only 4.7°. A possible explanation would be that the CS-tensor for cytidines (Stueber and Grant 2002) is more accurate than the CS-tensors provided for the other types of nucleotides (Duchardt et al. 2004; Ying et al. 2006). The comparison between the χ-angles determined by the $\Gamma^{DD,DD}_{C6H6,C1'H1'}$ and $\Gamma^{DD,DD}_{C8H8,C1'H1'}$ to the χ-angles obtained by analyzing the ^3J(C,H) couplings (Duchardt et al. 2004) (Table 2, Fig. 6C) yields an RMSD of 12.8°. Calculating the RMSD without G10, which is far out, reduces the RMSD to 7.3°. Finally, the correlation between the χ-angles extracted from a molecular dynamics trajectory and the χ-angles obtained by the analysis of the $\Gamma^{DD,DD}_{C6H6,C1'H1'}$ and $\Gamma^{DD,DD}_{C8H8,C1'H1'}$ yields an RMSD of 9.9°.

The results are in good agreement with the reference structure, the χ-angles determined from the $\Gamma^{CSA,DD}_{N1,C1'H1'}$ and $\Gamma^{CSA,DD}_{N9,C1'H1'}$ (Ennifar et al. 2000; Duchardt et al. 2004) and the χ-angles extracted from the ^3J(C,H) couplings. Furthermore, it has the following advantages over the $\Gamma^{CSA,DD}_{N1,C1'H1}$ ($\Gamma^{CSA,DD}_{N9,C1'H1'}$)-HCN method: The sensitivity of the experiment is better since the $\Gamma^{DD,DD}_{C6H6,C1'H1'}$ and $\Gamma^{DD,DD}_{C8H8,C1'H1'}$ rates are considerable larger than the $\Gamma^{CSA,DD}_{N1,C1'H1'}$ and $\Gamma^{CSA,DD}_{N9,C1'H1'}$ rates (Duchardt et al. 2004). Nucleotides assuming the syn conformation can be identified unambiguously. The main advantage of the new experiment is that it is independent of CSA and possible influences of other parameters such as the conformation itself on the N1(9) CS tensor do not have any effect on the results. In addition, the method is easy to implement since it is independent from the B_0-field.

SLD 30mer RNA

To test the applicability of the quantitative Γ-HCNCH experiment for larger RNAs it was applied to the SLD 30mer RNA which is part of the CVB3 cloverleaf RNA (Fig. 1B). For this RNA a high resolution solution structure determined by NMR (Ohlenschläger et al. 2004) is available (pdb 1RFR) and the resonance assignment of the C1′ and H1′ nuclei is known. We tested the method on an adenosine, uridine ^{13}C,^{15}N labeled sample. The spectra of the quantitative Γ-HCNCH reference and cross experiment are shown in Fig. 7. $\Gamma^{DD,DD}_{C6H6,C1'H1'}$ and $\Gamma^{DD,DD}_{C8H8,C1'H1'}$ are obtained from the intensities of the peaks from the cross and the reference spectra according to Eq. 4. In Fig. 8 the determined $\Gamma^{DD,DD}_{C6H6,C1'H1'}$ and $\Gamma^{DD,DD}_{C8H8,C1'H1'}$ rates were compared to the mean values for the χ-angle extracted from the NMR ensemble (pdb 1RFR). The black, blue and orange curves depict the predicted $\Gamma^{DD,DD}_{C6H6,C1'H1'}(\chi)$ and $\Gamma^{DD,DD}_{C8H8,C1'H1'}(\chi)$ relations assuming an isotropic τ_c of 4.76 ns (Ferner et al. to be published) (Eq. 2, Table 1). Since the

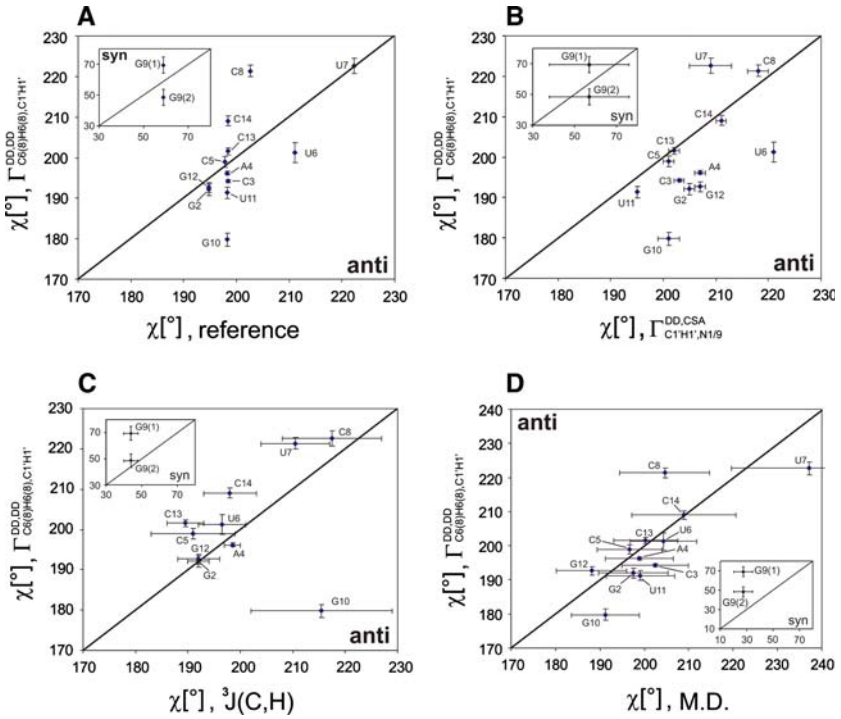

Fig. 6 (**A**) χ-angles extracted from the $\Gamma^{DD,DD}_{C6H6,C1'H1'}$ and $\Gamma^{DD,DD}_{C8H8,C1'H1'}$ compared to the χ-angles extracted from the X-ray structure (Duchardt et al. 2004). (**B**) Comparison between the χ-angles derived from the $\Gamma^{DD,DD}_{C6H6,C1'H1'}$ and $\Gamma^{DD,DD}_{C8H8,C1'H1'}$ to the χ-angles determined by $\Gamma^{CSA,DD}_{N1,C1'H1'}$ and $\Gamma^{CSA,DD}_{N9,C1'H1'}$ (Duchardt et al. 2004). (**C**) χ-angles obtained from the $\Gamma^{DD,DD}_{C6H6,C1'H1'}$ and $\Gamma^{DD,DD}_{C8H8,C1'H1'}$ compared to the χ-angles determined by the ^3J(C,H) couplings (Duchardt et al. 2004). (**D**) Average of χ-angles extracted from the molecular dynamics trajectory. There is only one possibility for the χ-angle lying close to the reference value (Ennifar et al. 2000; Duchardt et al. 2004) for each nucleotide in the anti position. In contrast, two values for the χ-angle remain possible for the nucleotide G9 which assumes the syn conformation

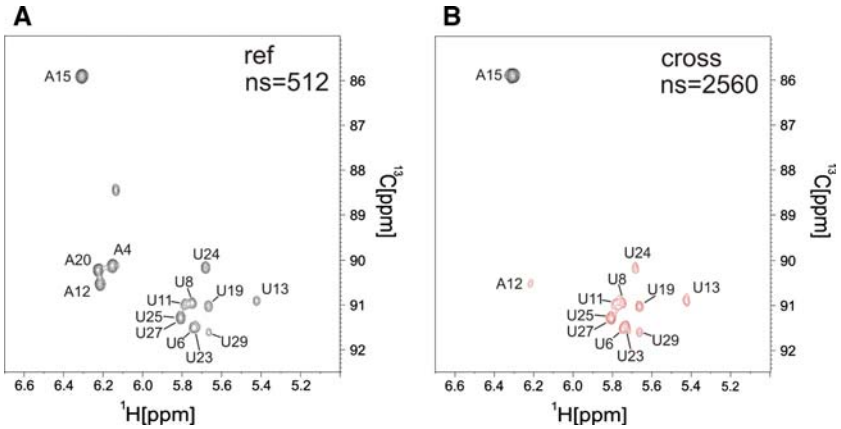

Fig. 7 Spectra of the quantitative Γ-HCNCH experiment for the 30mer RNA. The reference experiment is shown in (**A**), the cross experiment in (**B**). Negative signals are shown in red. The spectra were recorded on a 700 MHz spectrometer. The reference and the cross experiment were recorded using 44 increments in the C1′ dimension and 512 scans for each increment in the reference experiment. The cross experiment was recorded with 2560 scans per increment. T_M was set to 15 ms. The experiments were recorded within 69 h

30mer RNA has an extended shape, the effect of anisotropic rotational motion was investigated. The size and the orientation of the rotational diffusion tensor were determined with the NMR structure using the program HYDRONMR7 (Garcia de la Torre et al. 2000). Then, relying on the NMR structure the relative orientations of the bond vectors $\overrightarrow{C6H6}$ ($\overrightarrow{C8H8}$) and $\overrightarrow{C1'H1'}$ to the rotational diffusion tensor were determined.

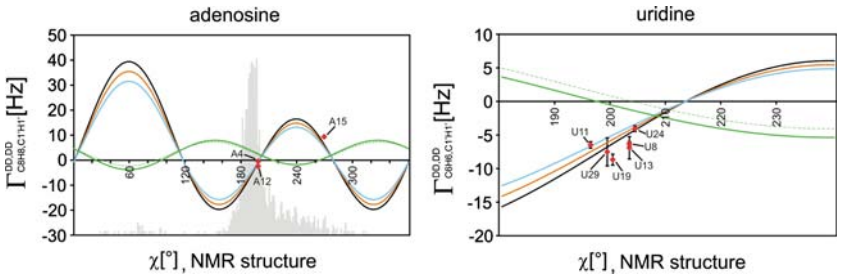

Fig. 8 $\Gamma^{DD,DD}_{C8H8,C1'H1'}(\chi)$ for adenosines and $\Gamma^{DD,DD}_{C6H6,C1'H1'}(\chi)$ for uridines assuming isotropic molecular tumbling, curves are shown for $(S^{DD,DD}_{C8H8,C1'H1'})^2$ and $(S^{DD,DD}_{C6H6,C1'H1'})^2$ equal to 0.8 (light blue), 0.9 (orange) and 1.0 (black). τ_c was set to 4.76 ns (Ferner and Schwalbe to be published) for the SLD 30mer at 310 K. In addition, the experimental $\Gamma^{DD,DD}_{C6H6,C1'H1'}$ and $\Gamma^{DD,DD}_{C8H8,C1'H1'}$ from the 30mer RNA are plotted against the reference χ-angles (Ohlenschläger et al. 2004) (red squares). $\Gamma^{CSA,DD}_{N1,C1'H1'}$ for pyrimidines and $\Gamma^{CSA,DD}_{N9,C1'H1'}$ for purines are illustrated as green solid (guanosine, cytidine) and dashed (adenosine, uridine) lines, respectively. The gray bars represent the χ-angle distribution in the RNA fraction of the large ribosomal subunit (PDB entry 1FFK (Ban et al. 2000))

Figure 9 shows the dependence of the $\Gamma^{DD,DD}_{C6H6,C1'H1'}$ and $\Gamma^{DD,DD}_{C8H8,C1'H1'}$ on the orientation of the bond vectors relative to the rotational diffusion tensor in the case of anisotropic axially symmetric tumbling (Schneider 1964; Hubbard 1969). Figure 9A shows the nomenclature that was used. A closer mathematical description is given in the supplementary material (S4). Figure 9B, C and D shows the effect of the anisotropy on the $\Gamma^{DD,DD}_{C6H6,C1'H1'}$ and $\Gamma^{DD,DD}_{C8H8,C1'H1'}$

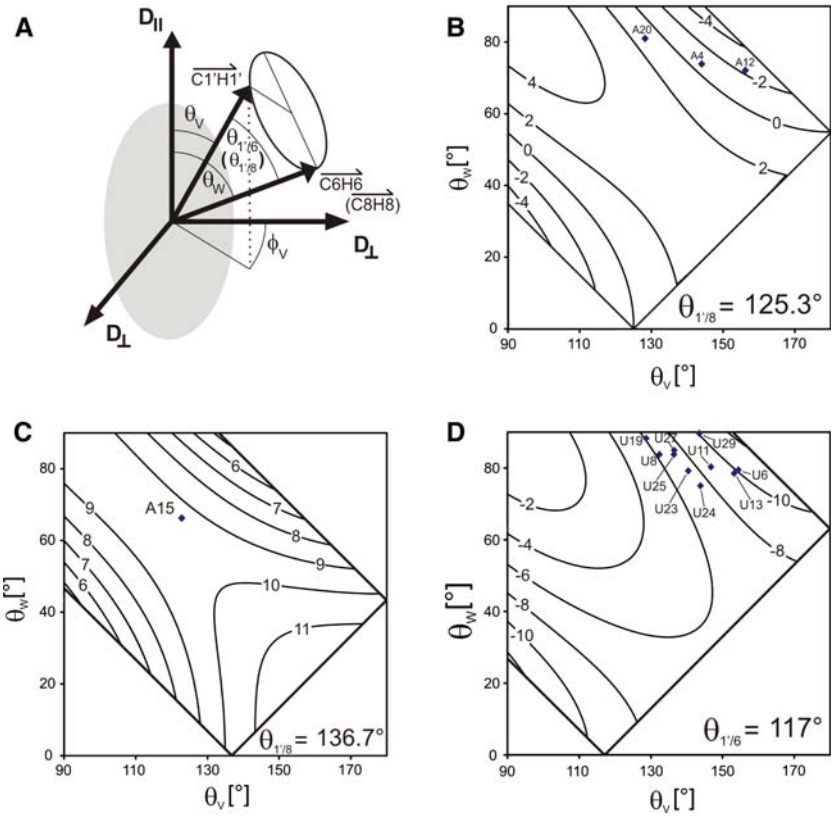

Fig. 9 Dependence of the $\Gamma^{DD,DD}_{C6H6,C1'H1'}$ and $\Gamma^{DD,DD}_{C8H8,C1'H1'}$ on the relative orientation to the axially symmetric rotational diffusion tensor for an anisotropy of 2.05 assuming an overall τ_c of 4.76 ns for the SLD 30mer. (**A**) Schematic drawing of the axially symmetric diffusion tensor with the nomenclature of the polar angles in relation to the rotational diffusion tensor. (**B**) $\Gamma^{DD,DD}_{C8H8,C1'H1'}$ dependence on the polar angles θ_V and θ_W for a projection angle $\theta_{1'/8}$ of 125.3°, which is the mean value of A20($\theta_{1'/8} = 125.3°$), A4($\theta_{1'/8} = 125.5°$) and A12($\theta_{1'/8} = 124.9°$) (**C**) $\Gamma^{DD,DD}_{C8H8,C1'H1'}$ dependence on the polar angles θ_V and θ_W for a projection angle $\theta_{1'/8}$ of 136.7° (A15). (**D**) $\Gamma^{DD,DD}_{C8H8,C1'H1'}$ dependence on the polar angles θ_V and θ_W for a projection angle of $\theta_{1'/6}$ of 117° (mean value for all uridines). For (**B**, **C** and **D**) the mean values for θ_V and θ_W for the adenosines and uridines of the SLD 30-mer RNA derived from the NMR structure ensemble (Ohlenschläger et al. 2004) are depicted as blue squares. For the simulated 2D-curves in (**B** and **D**) the mean values in $\theta_{1'/8}$ and $\theta_{1'/6}$ have been chosen in order to display the results in a compact form. In principle, each nucleotide has its own 2D-curve, which is dependent on $\theta_{1'/6}$ (pyrimidines) or $\theta_{1'/8}$ (purines)

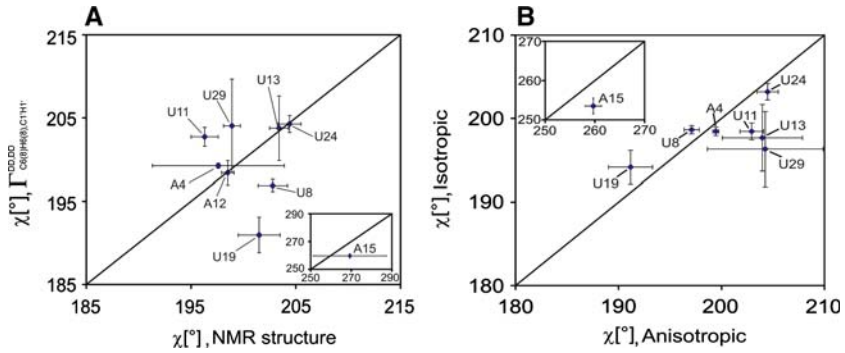

Fig. 10 (**A**) χ-angles extracted from the $\Gamma^{DD,DD}_{C6H6,C1'H1'}$ and $\Gamma^{DD,DD}_{C8H8,C1'H1'}$ compared to the χ-angles extracted from the NMR structure ensemble (Ohlenschläger et al. 2004). (**B**) Comparison between the χ-angles derived from the $\Gamma^{DD,DD}_{C6H6,C1'H1'}$ and $\Gamma^{DD,DD}_{C8H8,C1'H1'}$ assuming isotropic rotational diffusion and χ-angles determined by assuming anisotropic axially symmetric rotational diffusion with an anisotropy of 2.05

at a given projection angle $\theta_{C6H6,C1'H1'}$ $(\theta_{C8H8,C1'H1'})$ between the bond vectors $\overrightarrow{C6H6}(\overrightarrow{C8H8})$ and $\overrightarrow{C1'H1'}$. The extracted angles for θ_V and θ_W (see Fig. 9A) from the NMR structure show that most of the θ_W angles lie between 70° and 90° (blue squares in 9B, C, D). Since the rotational diffusion tensor is oriented almost parallel to the helix axes, it is evident that most of the vectors $\overrightarrow{C6H6}(\overrightarrow{C8H8})$ are oriented perpendicular to the diffusion tensor. A χ-angle of around 200° results in a θ_V-angle between 130° and 160° for most of the nucleotides. An exception is the nucleotide A15 that resides within the uCACGg tetraloop (Fig. 9C). Figure 9 shows that the effect of anisotropy on the $\Gamma^{DD,DD}_{C6H6,C1'H1'}$ and $\Gamma^{DD,DD}_{C8H8,C1'H1'}$ rates could be quite large for some θ_V and θ_W combinations. However, for the observed θ_V and θ_W combinations in the SLD 30mer this is not the case. Figure 10B shows the effect of rotational anisotropy on the extracted χ-angles. The figure shows that the anisotropic tumbling has the largest effect on the nucleotides U29 (8°) and A15 (6°) but the deviations between anisotropic and isotropic analysis is always <9°. In fact, the overall RMSD for the isotropic fitting is 6.9°. In conclusion, even for molecules with a large rotational diffusion anisotropy ($A \approx 2$), the assumption of isotropic tumbling still gives reasonable but not absolutely accurate results.

In order to define a high resolution structure the exact orientation of the anisotropy tensor has to be known. However, prediction of the axially symmetric diffusion tensor is quite precise even for a low resolution structure. Therefore, an iterative approach would be possible, in which the data of a molecule with extended shape are first analyzed isotropically and the outcoming structure is used to define a rotational diffusion anisotropy tensor. Subsequently, this tensor can be used to calculate a structure taking anisotropic rotational effects into account. This refinement procedure can be repeated until the structure is converged.

Finally, Fig. 10A gives a comparison between the χ-angles taken from the NMR structure and the χ-angles determined from the $\Gamma^{DD,DD}_{C6H6,C1'H1'}$ and $\Gamma^{DD,DD}_{C8H8,C1'H1'}$ rates and an anisotropic but axially symmetric diffusion tensor with an anisotropy of 2.05.

The correlation of the χ-angles is in a remarkable agreement with the reference structure with an overall RMSD of 5.8° proving that the method is also applicable for larger RNAs that show anisotropic rotational diffusion. The exact values are given in Table (S3) of the supplementary material.

In fact, the overall RMSD for the isotropic fitting is 6.9°, the RMSD for the anisotropic fitting is slightly better with 5.8°. The interpretation that the precision of the NMR structure might be the limiting factor for the RMSD is likely to be correct. Nevertheless, an RMSD of 5.8° is surprisingly good.

The incorporation of the χ-angle data into structural calculations should significantly improve the accuracy of RNA NMR structures since the analysis of the structure of the large ribosomal subunit (pdb ID 1FFK) shows that the χ-angles show a considerable spread of around 50° for purines and 30° for pyrimidines (see page 1). Therefore, it is not valid to preset the χ-angles to A-form conformation. The χ-angles have to be measured. NOEs on their own are most often not able to define the χ-angles with the desired accuracy, therefore additional constraints have to be obtained. The analysis of $\Gamma^{DD,DD}_{C6H6,C1'H1'}$ and $\Gamma^{DD,DD}_{C8H8,C1'H1'}$ cross-correlated relaxation rates is an easy to use, robust and precise method to get these constraints. The incorporation of χ-angles derived from cross correlated relaxation data into RNA structure calculations has already been described previously (Duchardt et al. 2004).

Conclusion

We have introduced a new method to determine the glycosidic torsion angle χ in RNA oligonucleotides relying on the analysis of CH,CH-dipole–dipole cross-correlated relaxation rates $\Gamma^{DD,DD}_{C6H6,C1'H1'}$ and $\Gamma^{DD,DD}_{C8H8,C1'H1'}$. This has been

shown exemplarily for the 14mer cUUCGg tetraloop RNA. The method allows to discriminate unambiguously between the syn and the anti conformation and is very accurate for nucleotides in the anti conformation. The provided $\Gamma^{DD,DD}$ (χ) parametrization is directly related to the known geometry of the nucleotides and is independent on the B_0-field strength. Therefore, the effect is also measurable at lower magnetic fields. Since the measured CH,CH dipolar cross-correlation effect scales up with the rotational correlation time τ_c this method is also suited to extract the χ-angles of larger RNA molecules as demonstrated for the SLD 30mer RNA.

Acknowledgements The paper is dedicated to Christian Griesinger. The work has been supported by the state of Hesse (Center for Biomolecular Magnetic Resonance) and the DFG (Sonderforschungsbereich: RNA-Ligand-Interactions). We wish to thank Oliver Ohlenschläger, Jens Wöhnert and Matthias Görlach for providing us with the 30mer RNA sample.

References

Allain FH, Varani G (1995) Structure of the P1 helix from group I self-splicing introns. J Mol Biol 250:333–353

Ban N, Nissen P, Hansen J, Moore PB, Steitz TA (2000) The complete atomic structure of the large ribosomal subunit at 2.4 A resolution. Science 289:905–920

Banci L, Bertini I, Felli IC, Hajieva P, Viezzoli MS (2001) Side chain mobility as monitored by CH–CH cross correlation: the example of cytochrome b5. J Biomol NMR 20:1–10

Batey RT, Inada M, Kujawinski E, Puglisi JD, Williamson JR (1992) Preparation of isotopically labeled ribonucleotides for multidimensional NMR spectroscopy of RNA. Nucleic Acids Res 20:4515–4523

Batey RT, Battiste JL, Williamson JR (1995) Preparation of isotopically enriched RNAs for heteronuclear NMR. Methods Enzymol 261:300–322

Boisbouvier J, Bax A (2002) Long-range magnetization transfer between uncoupled nuclei by dipole–dipole cross-correlated relaxation: a precise probe of beta-sheet geometry in proteins. J Am Chem Soc 124:11038–11045

Carlomagno T, Felli IC, Czech M, Fischer R, Sprinzl M, Griesinger C (1999) Transferred cross-correlated relaxation: application to the determination of sugar pucker in an aminoacylated tRNA-mimetic weakly bound to EF-Tu. J Am Chem Soc 121:1945–1948

Carlomagno T, Blommers MJ, Meiler J, Cuenoud B, Griesinger C (2001) Determination of aliphatic side-chain conformation using cross-correlated relaxation: application to an extraordinarily stable 2′-aminoethoxy-modified oligonucleotide triplex. J Am Chem Soc 123:7364–7370

Cromsigt J, van Buuren B, Schleucher J, Wijmenga S (2001) Resonance assignment and structure determination for RNA. Methods Enzymol 338:371–399

Duchardt E, Schwalbe H (2005) Residue specific ribose and nucleobase dynamics of the cUUCGg RNA tetraloop motif by MNMR 13C relaxation. J Biomol NMR 32:295–308

Duchardt E, Richter C, Ohlenschläger O, Görlach M, Wöhnert J, Schwalbe H (2004) Determination of the glycosidic bond angle chi in RNA from cross-correlated relaxation of CH dipolar coupling and N chemical shift anisotropy. J Am Chem Soc 126: 1962–1970

Emsley L, Bodenhausen G (1992) Optimization of shaped selective pulses for NMR using a quaternion description of their overall propagators. J Magn Reson 97:135–148

Ennifar E, Nikulin A, Tishchenko S, Serganov A, Nevskaya N, Garber M, Ehresmann B, Ehresmann C, Nikonov S, Dumas P (2000) The crystal structure of UUCG tetraloop. J Mol Biol 304:35–42

Feller SE, Zhang Y, Pastor RW, Brooks BR (1995) Constant pressure molecular dynamics simulation: the Langevin piston method. J Chem Phys 103:4613–4621

Felli I, Richter C, Griesinger C, Schwalbe H (1999) Determination of RNA sugar pucker mode from cross-correlated relaxation in solution NMR spectroscopy. J Am Chem Soc 121:1956–1957

Ferner J, Duchardt E, Villa A, Stock G, Schwalbe H (to be published)

Fiala R, Jiang F, Sklenář V (1998) Sensitivity optimized HCN and HCNCH experiments for 13C/15N labeled oligonucleotides. J Biomol NMR 12:373–383

Fiala R, Munzarova ML, Sklenar V (2004) Experiments for correlating quaternary carbons in RNA bases. J Biomol NMR 29:477–490

Foloppe N, MacKerell AD Jr (2000) All-atom empirical force field for nucleic acids: I. Parameter optimization based on small molecule and condensed phase macromolecular target data. J Comp Chem 21:86–104

Fürtig B, Richter C, Wöhnert J, Schwalbe H (2003) NMR-spectroscopy of RNA. ChemBioChem 4:936–962

Fürtig B, Richter C, Bermel W, Schwalbe H (2004) New NMR experiments for RNA nucleobase resonance assignment and chemical shift analysis of an RNA UUCG tetraloop. J Biomol NMR 28:69–79

Garcia de la Torre J, Huertas ML, Carrasco B (2000) HYDRONMR: prediction of NMR relaxation of globular proteins from atomic-level structures and hydrodynamic calculations. J Magn Reson 147:138–146

Geen HF, Freeman R (1991) Band-selective radiofrequency pulses. J Magn Reson 93:93–141

Hubbard PS (1969) Nonexponential relaxation of three-spin systems in nonspherical molecules. J Chem Phys 51:1647

Ilin S, Bosques C, Turner C, Schwalbe H (2003) Gamma-HMBC: an NMR experiment for the conformational analysis of the o-glycosidic linkage in glycopeptides. Angew Chem Int Ed 42:1394–1397

Jorgensen WL, Chandrasekhar J, Madura JD, Impey RW, Klein ML (1983) Comparison of simple potential functions for simulating liquid water. J Chem Phys 79: 926–935

Kay L, Keifer P, Saarinen T (1992) Pure absorption gradient enhanced heteronuclear single quantum correlation spectroscopy with improved sensitivity. J Am Chem Soc 114:10663–10665

Kloiber K, Schuler W, Konrat R (2002) Automated NMR determination of protein backbone dihedral angles from cross-correlated spin relaxation. J Biomol NMR 22:349–363

MacKerell Jr AD, Banavali NK (2000) All-atom empirical force field for nucleic acids: II. Application to molecular dynamics simulations of DNA and RNA in solution. J Comp Chem 21:105–120

Marion D, Ikura M, Tschudin R, Bax AJ (1989) Rapid recording of 2D NMR spectra without phase cycling. Application to the study of hydrogen exchange in proteins. J Magn Reson 85:393–399

Markwick PR, Sprangers R, Sattler M (2005) Local structure and anisotropic backbone dynamics from cross-correlated NMR relaxation in proteins. Angew Chem Int Ed 44:3232–3237

Millet O, Chiarparin E, Pelupessy P, Pons M, Bodenhausen G (1999) Measurement of relaxation rates of NH and Ha backbone protons

in proteins with tailored initial conditions. J Magn Reson 139:434–438

Munzarova ML, Sklenar V (2003) DFT analysis of NMR scalar interactions across the glycosidic bond in DNA. J Am Chem Soc 125:3649–3658

Nikonowicz EP, Sirr A, Legault P, Jucker FM, Baer LM, Pardi A (1992) Preparation of 13C and 15N labelled RNAs for heteronuclear multi-dimensional NMR studies. Nucleic Acids Res 20:4507–4513

Ohlenschläger O, Wöhnert J, Bucci E, Seitz S, Hafner S, Ramachandran R, Zell R, Görlach M (2004) The structure of the stemloop D subdomain of coxsackievirus B3 cloverleaf RNA and its interaction with the proteinase 3C. Structure 12:237–248

Pelupessy P, Chiarparin E, Ghose R, Bodenhausen G (1999) Efficient determination of angles subtended by C(alpha)–H(alpha) and N–H(N) vectors in proteins via dipole–dipole cross-correlation. J Biomol NMR 13:375–380

Quant S, Wechselberger R, Wolter M, Wörner K-H, Schell P, Engels J, Griesinger C, Schwalbe H (1994) Chemical synthesis of 13C-labelled monomers for solid-phase and template controlled enzymatic synthesis of DNA and RNA oligomers. Tetrahedron Lett 35:6649–6652

Ravindranathan S, Kim CH, Bodenhausen G (2003) Cross correlations between 13C–1H dipolar interactions and 15N chemical shift anisotropy in nucleic acids. J Biomol NMR 27:365–375

Reif B, Hennig M, Griesinger C (1997) Direct measurement of angles between bond vectors in high-resolution NMR. Science 276:1230–1233

Richter C, Griesinger C, Felli I, Cole PT, Varani G, Schwalbe H (1999) Determination of sugar conformation in large RNA oligonucleotides from analysis of dipole–dipole cross correlated relaxation by solution NMR spectroscopy. J Biomol NMR 15:241–250

Richter C, Reif B, Griesinger C, Schwalbe H (2000) NMR spectroscopic determination of angles α and ζ in RNA from CH–dipolar coupling, P-CSA cross-correlated relaxation. J Am Chem Soc 122:12728–12731

Roehrl MH, Heffron GJ, Wagner G (2005) Correspondence between spin-dynamic phases and pulse program phases of NMR spectrometers. J Magn Reson 174:325–330

Schneider H (1964) Z Naturforsch Teil A 19:510

Schwalbe H, Marino JP, King GC, Wechselberger R, Bermel W, Griesinger C (1994) Determination of a complete set of coupling constants in 13C-labeled oligonucleotides. J Biomol NMR 4:631–644

Schwalbe H, Carlomagno T, Hennig M, Junker J, Reif B, Richter C, Griesinger C (2001) Cross-correlated relaxation for measurement of angles between tensorial interactions. Methods Enzymol 338:35–81

Shaka AJ, Barker PB, Freeman RJ (1985) Computer-optimized decoupling scheme for wideband applications and low-level operation. J Magn Reson 64:547–552

Sklenar V, Peterson RD, Rejante MR, Feigon J (1993a) Two- and three-dimensional HCN experiments for correlating base and sugar resonances in 15N,13C-labeled RNA oligonucleotides. J Biomol NMR 3:721–727

Sklenar V, Rejante MR, Peterson RD, Wang E, Feigon J (1993b) Two-dimensional triple-resonance HCNCH experiment for direct correlation of ribose H1′ and base H8, H6 protons in 13C,15N-labeled RNA oligonucleotides. J Am Chem Soc 115:12181–12182

Sklenar V, Dieckmann T, Butcher SE, Feigon J (1998) Optimization of triple-resonance HCN experiments for application to larger RNA oligonucleotides. J Magn Reson 130:119–124

Stueber D, Grant DM (2002) 13C and (15)N chemical shift tensors in adenosine, guanosine dihydrate, 2′-deoxythymidine, and cytidine. J Am Chem Soc 124:10539–10551

Sychrovsky V, Muller N, Schneider B, Smrecki V, Spirko V, Sponer J, Trantirek L (2005) Sugar pucker modulates the cross-correlated relaxation rates across the glycosidic bond in DNA. J Am Chem Soc 127:14663–14667

Trantirek L, Stefl R, Masse JE, Feigon J, Sklenar V (2002) Determination of the glycosidic torsion angles in uniformly 13C-labeled nucleic acids from vicinal coupling constants 3J(C2)/4-H1′ and 3J(C6)/8-H1′. J Biomol NMR 23:1–12

Tugarinov V, Kay LE (2004) 1H,13C-1H,1H dipolar cross-correlated spin relaxation in methyl groups. J Biomol NMR 29:369–376

Varani G, Aboul-ela F, Allain FH-T (1996) NMR investigation of RNA structure. Prog Nucl Magn Reson Spectrosc 29:51–127

Varani G, Tinoco I Jr (1991) RNA structure and NMR spectroscopy. Q Rev Biophys 24:479–532

Vugmeyster L, Pelupessy P, Vugmeister BE, Abergel D, Bodenhausen G (2004) Cross-correlated relaxation in NMR of macromolecules in the presence of fast and slow internal dynamics. CR Phys 5:377–386

Wang T, Frederick KK, Igumenova TI, Wand AJ, Zuiderweg ER (2005) Changes in calmodulin main-chain dynamics upon ligand binding revealed by cross-correlated NMR relaxation measurements. J Am Chem Soc 127:828–829

Wijmenga SS, van Buuren BNM (1998) The use of NMR methods for conformational studies of nucleic acids. Prog Nucl Magn Reson Spectrosc 32:287–387

Ying J, Grishaev A, Bax A (2006) Carbon-13 chemical shift anisotropy in DNA bases from field dependence of solution NMR relaxation rates. Magn Reson Chem 44:302–310

Zwahlen C, Vincent SJ (2002) Determination of (1)H homonuclear scalar couplings in unlabeled carbohydrates. J Am Chem Soc 124:7235–7239